Multi-strand β-sheet of Alzheimer Aβ(1–40) folds to β-strip helix: Implication for protofilament formation

Steven Hayward[a*] and Akio Kitao[b*]

[a] D'Arcy Thompson Centre for Computational Biology, School of Computing Sciences, University of East Anglia, Norwich, U.K.

[b] School of Life Science and Technology, Tokyo Institute of Technology, 2-12-1 Ookayama, M6-13, Meguro, Tokyo 152-8550, Japan

*Correspondence to:

Dr Steven Hayward, D'Arcy Thompson Centre for Computational Biology, School of Computing Sciences, University of East Anglia, Norwich, U.K. steven.hayward@uea.ac.uk

Professor Akio Kitao, School of Life Science and Technology, Tokyo Institute of Technology, 2-12-1 Ookayama, M6-13, Meguro, Tokyo 152-8550, Japan.

akitao@bio.titech.ac.jp

Multi-strand β-sheet of Alzheimer Aβ(1–40) folds to β-strip helix: Implication for protofilament formation

ABSTRACT

X-ray fibre diffraction experiments on Alzheimer Aβ(1-40) fibrils (Fraser et al. Biochemistry 31, 1992; Malinchik et al. Biophysical Journal, 74, 1998) indicated protofilaments with tilted β-strands rather than strands oriented perpendicular to the fibril axis as is usually interpreted from cross-β patterns. The protofilament width and tilt angle determined by these experiments were used to predict a β-strip helix model – a β-helix-like structure in which multiple identical polypeptide molecules assemble in-register to form a helical sheet structure such that the outer strands 1 and m join with a register shift t – with m=11 and t=22. Starting from untwisted β-sheets comprising 10, 11 and 12 strands, multiple explicit solvent Molecular Dynamics simulations were performed to determine whether the sheets form β-strip helices matching the dimensions of the experimentally measured protofilament. In the simulations, the predicted 11-strand sheets curled up to form a closed β-strip helix like structure with dimensions matching experimental values, whereas the 10- and 12-strand sheets did not form a closed helical structure. However, the 12-strand structure did show similarity to a cross-β structure determined by a solid-state NMR experiment. The 11-strand β-strip helix resembles a trans-membrane β-barrel which could explain the ability of small oligomers of Aβ(1-40) to form toxic ion channels. A further consequence of opposite sides of the 11-strand strip coming together at a register shift of 22 is end-to-end joins between neighbouring β-strip helices, resulting in a protofilament that keeps growing in both directions.

Keywords: molecular dynamics simulation, cross-β, shear number, β-helix, β-barrel.

Introduction

Amyloid refers to an alternative protein conformation that all proteins seem to be able to adopt given the right conditions (Sipe and Cohen, 2000). It is a misfolded form that in contrast to the native form is stable against denaturants. The formation of amyloid is the cause of a number of well-known chronic diseases (Buxbaum and Linke, 2012; Eisenberg and Jucker, 2012) including type II diabetes, Huntington's disease, Parkinson's and Alzheimer's. Prions are also considered to be amyloid (Ritter et al., 2005). The mature form of amyloid comprises unbranched fibrils that are thought to comprise in-register parallel β-sheet (Shewmaker, McGlinchey, & Wickner, 2011; Shinchuk et al., 2005; Wickner, Shewmaker, Kryndushkin, & Edskes, 2008), although antiparallel β-sheet has also been characterised (Lendel et al., 2014; Rodriguez et al., 2015; Sawaya et al., 2007; Serra-Batiste et al., 2016). It has become widely accepted that amyloid fibrils comprise β-sheet in the cross-β configuration, that is with the β-strands running perpendicular to the fibril axis direction. Although cross-β is common to many amyloid fibrils there is a considerable conformational diversity amongst amyloid fibrils (Toyama and Weissman, 2011) and β-helical structures have also been proposed (Hayward and Milner-White, 2017; Makin and Serpell, 2005). The HET-s(218-289) prion protein (Wasmer et al., 2008) provides an example with fibril subunits formed from single-strand β-helices that join end-to-end. Single-strand β-helices are approximately cross-β, but for β-helices comprising more than one strand folded into a β-helical structure, such as in β-strip helices, (Hayward and Milner-White, 2017) strands cannot be perfectly cross-β.

The Molecular Dynamics (MD) simulations presented here are based on the results of X-ray fibre diffraction experiments carried out in the Kirschner group by Fraser et al. (Fraser et al., 1992) and Malinchik et al.(Malinchik, Inouye, Szumowski, & Kirschner, 1998) on Alzheimer Aβ(1-40) fibrils. The result of these experiments, in contrast to the more recent

solid-state NMR studies(Lu et al., 2013; Lührs, et al., 2005; Paravastu, Leapman, Yau, & Tycko, 2008; Petkova et al., 2002), was that the β-strands in the protofilament were tilted to the protofilament axis direction. In the work by Fraser et al the (200) reflections of the orthogonal unit cell, corresponding to the perpendicular distance between chains, were off the meridian, whereas the (210) reflections were on the meridian. This result showed that the strands were tilted by 35.6° to the expected cross-β configuration; that is at an angle of 54.4° to the fibril axis direction. In the study by Malinchik et al. both (200) and (210) reflections were on the meridian which was attributed to a relative enhancing of the on-meridional reflections relative to the off-meridional reflections due to cylindrical averaging and disorder within the fibril. The conclusion was that the strands were tilted with respect to perpendicular to the protofilament axis direction. Although the cross-β configuration appears to be the dominant form for amyloid it has also been established that there is a great deal of conformational diversity depending on variant and experimental conditions. From the perspective of understanding how the Aβ amyloid forms in Alzheimer disease (AD), only certain variants and environmental conditions are relevant. The importance of the study by Malinchik et al. may lie in the careful process used to grow the fibrils from low concentrations of soluble monomeric peptide : "*The significance of our current study arises because…the assembly process itself (from soluble peptide to insoluble fibers) may simulate a portion of the pathophysiological process leading to fibril formation in AD brains*."

Hayward and Milner-White (HMW) (Hayward and Milner-White, 2017) extended the theory for the shear number (McLachlan, 1979; Murzin, Lesk, & Chothia, 1994) in β-barrels for application to β-helices and homomeric β-barrels and β-helices. In this development, the minimal unit is the "β-strip" from which the whole helical structure can be constructed via the symmetry operations of the *n*-fold rotational axis which is the helical axis. The development led to a set of equations that relate geometrical quantities, such as helical radius,

4

r, height per turn, h, and angle between the strand direction and the helical axis direction, α, to quantities such as, n, the number of β-strips, m, the number of strands in the β-strip, and t the register shift between neighbouring β-strips:
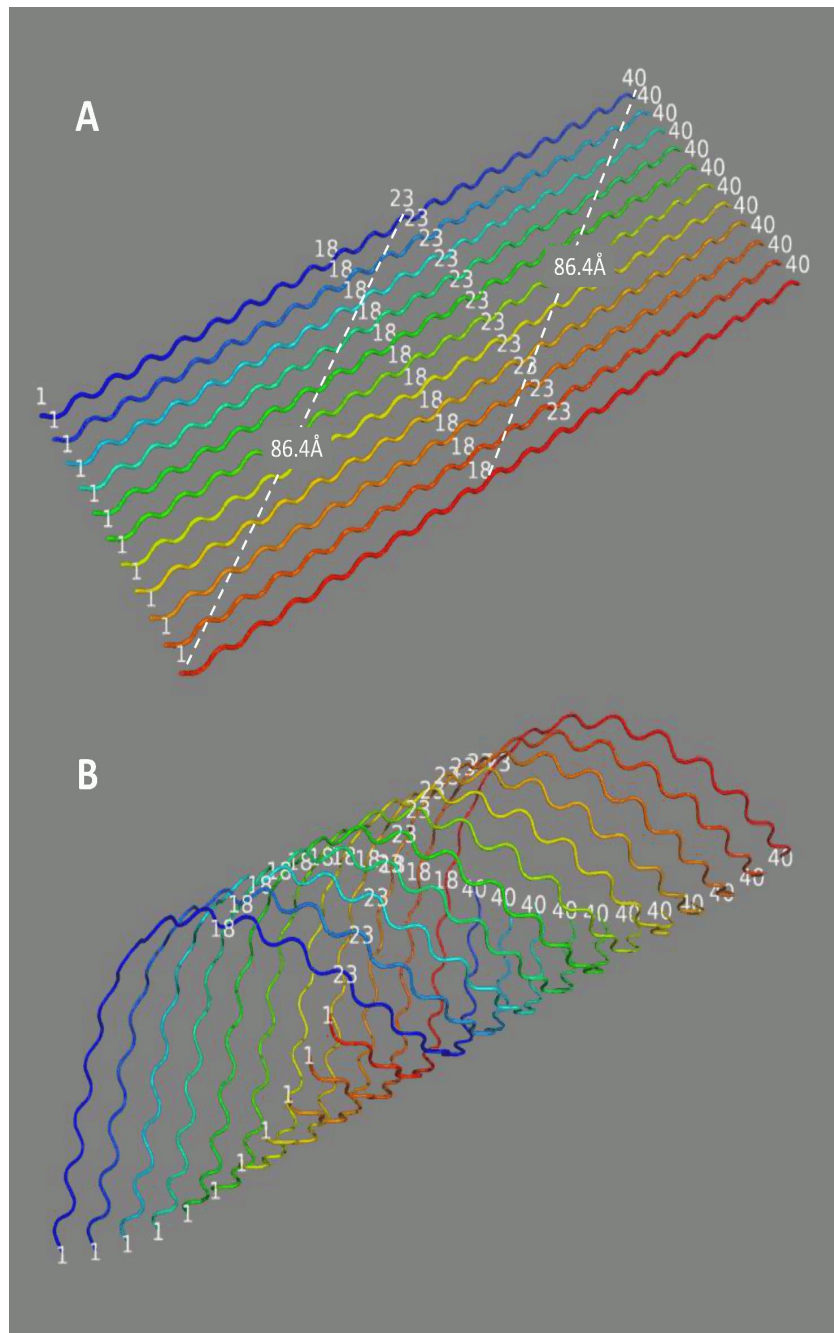
$$\frac{t}{m} = \frac{b}{a}\tan\alpha \tag{1a}$$

$$h = \frac{b}{a}2\pi r\left(\frac{t}{m}\right)^{-1} \tag{1b}$$

$$nm = \frac{2\pi rh}{b\sqrt{(2\pi r)^2 + h^2}} \tag{1c}$$

where a and b are constants and are set here to 3.3 Å and 4.8 Å respectively (see Methods Section). In the X-ray fibre diffraction experiments on the Aβ(1-40) fibrils by Fraser et al. and Malinchik et al. the protofilament dimensions r and α were found to be 14-15 Å and 54.4°, respectively. Assuming a helix of circular cross-section, Equations (1) give $t/m = 2.0$, $h = 63.0 – 67.5$ Å and $nm = 10.7 – 11.4$. Amyloid is widely considered to exist as parallel in-register β-sheet (Shewmaker, et al., 2011; Shinchuk, et al., 2005; Wickner, et al., 2008) and site-directed spin labelling experiments on Aβ(1-40) have shown that the strands are parallel and in register (Torok et al., 2002). As described in HMW this suggests the protofilament subunit comprises a single strip ($n = 1$) of in-register strands folded to a "β-strip helix", where at the join between the two outermost strands the register shift is t. If $n = 1$ then $m = 10.7 – 11.4$, but as m must be an integer, this implies $m = 11$ and $t = 22$ (t must be even). With $m = 11$ and $t = 22$ we can use the equations in HMW to find the helical dimensions of the "experimental β-strip helix model" which are: $r = 14.3$ Å, $\alpha = 54.0°$ and $h = 65.3$ Å. The underlying assumption is that the Aβ(1-40) protofilament in these experiments is formed from β-strip helices. Thus the experimental β-strip helix model is a β-strip helix consistent with the experimental measurements. Figure 1 (B) shows the backbone trace of the experimental β-strip helix model constructed as described in the Methods section. Fraser et

5

al. also saw a weak reflection at 57 Å on the meridian which they suggested might be due to an axially repeating unit comprising 12 strands. The calculation above, which derives from knowledge of r and α only, suggests a β-strip helix of 11 strands and a length of approximately 60 Å (see HMW for further details), which, if it formed the repeating protofilament subunit, might explain the 57 Å meridional reflection.

Figure 1

(A) Flat β-sheet with 11 straight in-register strands of 40 residues. (B) "Experimental β-strip helix model", the β-strip helix of circular cross-section consistent with the X-ray fibre diffraction results. It corresponds to the sheet shown in (A) where residues 23-40 in chain A (blue) hydrogen bond to residues 1-18 in chain K (red).

MD simulations of Alzheimer Aβ(1-40) and Aβ(1-42) have been performed by a number of groups as reported in the thorough review by Nasica-Labouze et al. (Nasica-Labouze et al., 2015). There are reports of MD simulations on higher order assemblies of Aβ(1-40) or Aβ(1-42) which start from known NMR structures for simulation of the aggregation process or effect of a lipid membrane environment. For example, implicit-solvent simulations (Barz, Olubiyi, & Strodel, 2014) have been used to study the assembly process starting with 20 NMR monomer structures of Aβ(1-40) (Coles, Bicknell, Watson, Fairlie, & Craik, 1998). All-atom explicit-solvent simulations on truncated Aβ(1-40) protofilament structures determined by solid state NMR (Lührs, et al., 2005; Petkova, Yau, & Tycko, 2006) approaching or embedded in lipid bilayers have also been reported (Jang et al., 2010; Tofoleanu, Brooks, & Buchete, 2015). There are no reports, however, of MD simulations performed to understand the strain of the Aβ(1-40) protofilament structure reported by Fraser et al. and Malinchik et al..
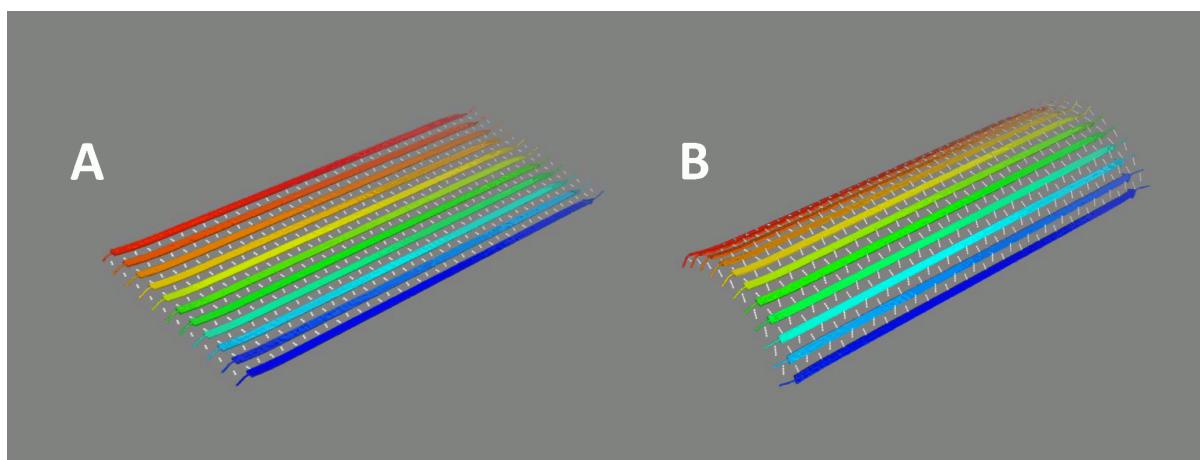
The cover image of Proteins Vol 85 Issue 10 (Hayward and Milner-White, 2017), taken from HMW, shows a paper model starting as a flat sheet curling up to form a helical structure. Here we present explicit-solvent MD simulations starting from untwisted β-sheets of 10-, 11- and 12-strands. It is important to appreciate that the aim here is not to simulate the folding process from an artificial structure, but rather to determine whether, from limited information (in-register strands with parallel β-sheet hydrogen bonding), the resulting stable structure is a β-strip helix with dimensions close to those experimentally measured. Should this be confirmed for the predicted 11-strand sheet then it would support the hypothesis that the experimental β-strip helix is a good model for the protofilament subunit.

Methods

Construction of β-sheets for simulation

Using an in-house program, polyalanine models can be constructed with standard bond lengths, bond angles, ω torsion angles and desired (ϕ, ψ) angles. Sheets for simulation were constructed from straight untwisted strands (with exactly 180° rotation about the strand helical axis per residue) for which excellent inter-strand hydrogen bonding can be achieved along the whole length. Such a strand with standard bond angles, standard ω torsions angles,

Figure 2

(A) Starting structure that has straight strands and a flat surface. (B) Starting structure with straight strands and a curved surface.

and repeating (ϕ, ψ) angles satisfies the equation $\psi = -2\arctan(0.92\tan(\phi/2))$ (Hayward and Milner-White, 2011). A straight strand of 40 alanine residues was constructed using the angles, (-120°, 115.8°), which satisfy this equation and also are close to the average (ϕ, ψ) angles in parallel β-sheet. A duplicate strand was created and brought into optimal interaction with the original using rigid body transformations (Hayward and Milner-White, 2011). The resulting untwisted two-strand β-sheet comprised hydrogen bonds along its whole length. Repeating this process a multi-strand sheet could be created. If the rigid body transformation involved only translation then the sheet is perfectly flat as shown in Figure 2 (A). If in

addition to translations, rotations were used then a slightly curved, but still untwisted sheet arose as shown in Figure 2(B). The side-chains corresponding to the wild-type human Alzheimer Aβ(40) protein were placed using SQRWL (Krivov, Shapovalov, & Dunbrack, 2009). Sheets of 10, 11 and 12 strands were created.

This procedure ensures that there is neither a twisting bias nor a bias caused by a particular pattern of hydrogen bonds introduced into the starting structures.

Modelling a β-strip helix

A β-strip helix comprises m identical strands in register but the outer strands, strand 1 and strand m meet with a register shift t (see Figure 1 (B)). Specifying m and t (t must be an even number) determines the helical radius, r, and height per turn, h, or vice-versa as per the equations given previously by HMW. A structure constructed with these values of r and h will be a closed β-strip helix; that is the two outer strands align at the desired register shift of t. There are two constants that relate to C^{α} atom spacing: the direct distance, a, between successive C^{α} atoms along the "strand helix", the helix that follows the strand direction, and the direct distance, b, between aligned C^{α} atoms along the "neighbour helix", the helix that crosses the strand helix at right angles. Here, as in HMW, we set $a = 3.3$ Å and $b = 4.8$ Å. The parametric equation of a helix was used to place C^{α} atoms at the appropriate spacing on a strand. In Supplementary Material we describe a method to place a neighbouring strand and in this way to build up the whole β-strip helix. The experimental β-strip helix model can be constructed in this way.

β-strip helices with end-to-end join

β-strip helices can join end-to-end by the association of same pair of sequence segments that come together to stabilise the β-strip helix. As shown in Supplementary Material, for this to be able to happen the condition $L \leq 2t \leq 2(L-1)$ must be satisfied, where L is the length of the strand. As also shown in Supplementary Material, the length of the gap, g, between the end of one chain and the start of the next as a shift in the number of residues, is given by $g = 2t - L + 1$. In Supplementary Material it is also shown how to construct a model of a protofilament comprising β-strip helices joined end-to-end.

Determination of helical dimensions of final structures - fitted β-strip model

In order to determine the approximate helical geometry of the final structures, the root mean-square deviation (RMSD) between the C^{α} atoms of the final structure and a constructed β-strip helix of the same number of strands was minimised (using Matlab's "fminsearch" function) in the parameter space of r and h, i.e. assuming a β-strip helix of circular cross-section. In this process the distances between successive C^{α} atoms along a strand and between strands were maintained at 3.3 Å and 4.8 Å, respectively. The same number of strands was used as in the structure being modelled but closure of the strip was not imposed. The resulting structure will be referred to as a "fitted β-strip model".

Inter-strand register shift based on residue contact analysis

Labelling strands A to K for the 11-strand case, we measure the "inter-strand register shift" between chains A and K (or J for 10-strands; L for 12 strands) in the following way. For each residue on strand A, a list of contacting residues on strand K was compiled. The register shift between each residue on A and all its contacting residues on K was then calculated to give a list of register shifts for each residue on A. The lists from all residues on A were combined and the mean of this combined list taken to give the inter-strand register shift between A and

11

K. This was calculated at each frame and was performed not just between the outermost strands but between all pairs of the two outermost strands on either side of the sheet. "Contact" between residue i and residue j means any atom (including hydrogen atoms) of residue i is within 3.5 Å of any atom of residue j.

MD protocols

All MD simulations were performed by AMBER16 (D.A. Case, A.W. Goetz, Lin, Omelyan, & R.C. Walker, 2016) on 10-, 11- and 12-strand sheets for 1 or 2 μs in explicit solvent as listed in Table I. As the starting structure, we used either the flat or curved sheet. Charged groups, NH_3 and COO (NH3/COO), were used for the N- and C-termini for the first three simulations in Table I, and neutral acetyl and N-methyl groups (ACE/NME) were selected for the rest. The latter treatment was used to assess the effect of terminal charges, however, no significant effects were observed as shown in the Results section. The AMBER ff14SB force field was used for the peptides (Maier et al., 2015).

TABLE I Details of MD simulations performed

Simulation name comprises following information: number of strands_simulation box type_Curved or Flat starting structure_neutral or charged terminal groups.

Simulation name	Nº of chains	Box type	Nº of atoms	Starting structure	Terminal groups	Simulation time
10_cuboid_C_chg	10	Cuboid	67,666	Curved	NH3/COO	2μs
11_cuboid_C_chg	11	Cuboid	97,720	Curved	NH3/COO	2μs
11_cube_C_chg	11	Cube	352,263	Curved	NH3/COO	1μs
11_cube_C_ntl	11	Cube	378,039	Curved	ACE/NME	2μs
11_cube_F_ntl	11	Cube	380,427	Flat	ACE/NME	1μs
12_cube_F_ntl	12	Cube	376,312	Flat	ACE/NME	1μs

Two types of periodic boundary boxes, cuboid and cube, were used. The cuboid was utilized to minimize the number of solvent molecules in the box, whereas the cube is able to

minimize possible artefacts caused by the reorientation of the peptides during a long MD

simulation. As shown in Results, we did not see any significant difference caused by the

shape of the box. In the cuboid case, we first energy minimized for 200 steps with the

implicit solvent model, Generalized Born/Surface Area (GB/SA), with the CUDA version of

the Pmemd module (Gotz et al., 2012). Then, the system was equilibrated with GB/SA-MD

for 1 ns with positional restraints imposed on heavy atoms (force constant: 0.1 kcal/molÅ^2)

and for an additional 1 ns with the restraints on C$^\alpha$ atoms only. Then, 100 ns of GB/SA-MD

was conducted without restraints. During this period, an initial conformational change from a

relatively flat structure to a more curved one was observed. The final structure of the GB/SA-

MD was solvated in a cuboid box, so that there was at least a 10 Å gap between the peptides

and the boundary. The initial box sizes for 10_cuboid_C_chg and 11_cuboid_C_chg were

135×71×84 and 144×90×90 Å^3, respectively. For the cubic boundary, the peptides were

solvated in a cube with the same gap condition. The initial boxes sizes for 11_cube_C_chg,

11_cube_C_ntl, 11_cube_F_ntl, and 12_cube_F_ntl were 157^3, 161^3, 161^3 and 161^3 Å^3,

respectively. The number of atoms in each box is given in Table I. The SPC/Eb model

(Takemura and Kitao, 2012) was used for water and Joung/Cheatham parameters (Joung and

Cheatham, 2008) for KCl ions which were distributed in the box to neutralise it and impose

0.14 M ionic strength to the system. After energy minimization, 1 ns of MD simulation was

performed at 1 atm and 300 K with positional restraints imposed on main chain N, C$^\alpha$, C′,

and O atoms (the force constant: 1.0 kcal/molÅ^2) in 10_cuboid_C_chg, 11_cuboid_C_chg

and 11_cube_C_chg. In other cases, 5 ns of MD simulation was performed with positional

restraints imposed on N, C$^\alpha$, and C′ by gradually weakening the force constant from 1.0 to

0.01 kcal/molÅ^2. All the molecular dynamics simulations were performed using the GPU

implementation of Pmemd module(Le Grand, Gotz, & Walker, 2013). Isothermal-isobaric

conditions were achieved by a Langevin thermostat (Sindhikara, Kim, Voter, & Roitberg,

2009) and a Berendsen barostat (Berendsen, Postma, van Gunsteren, Di Nola, & Haak, 1984).
Equations of motion were integrated with a time step of 2 fs. The long-range Coulomb energy
was evaluated using the particle mesh Ewald method (Essmann et al., 1995). After restraints-
MD, MD simulation without restraints was conducted for 1 or 2 μs, and the generated
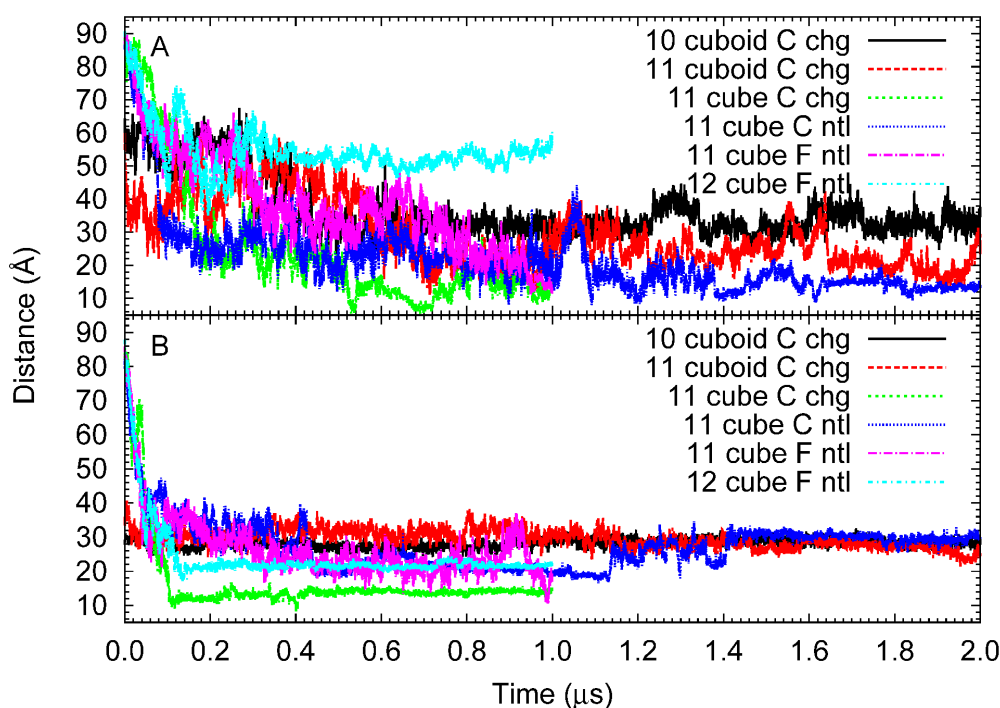trajectories were used for the analysis.

Simulations were performed on a Xeon E5-2670 with a Tesla K20 GPU. A 2 μs
cubic box simulation took approximately 300 days.

Results

Simulations with 11-strands

Analysis of trajectories

In all cases the strip spontaneously curls up to form a β-strip helix. In all cases the β-strip is a
right-handed helix and a significant proportion of β-sheet hydrogen-bonding is maintained as
shown in Figure 4 (A). Given that a sheet has two surfaces, arbitrarily denoted "A" and "B",
there are two possible right-handed helices that could arise: one with surface A on the outside
of the helix and surface B on the inside or vice-versa. We can distinguish which of the two
possible right-handed helices our β-strip helices are by identifying which residues are on the
outside of the helix. The red characters at the bottom of Figure 4(C) show the residues on the
outside of the helix, which are common to all the MD results. Due to disorder at the ends this
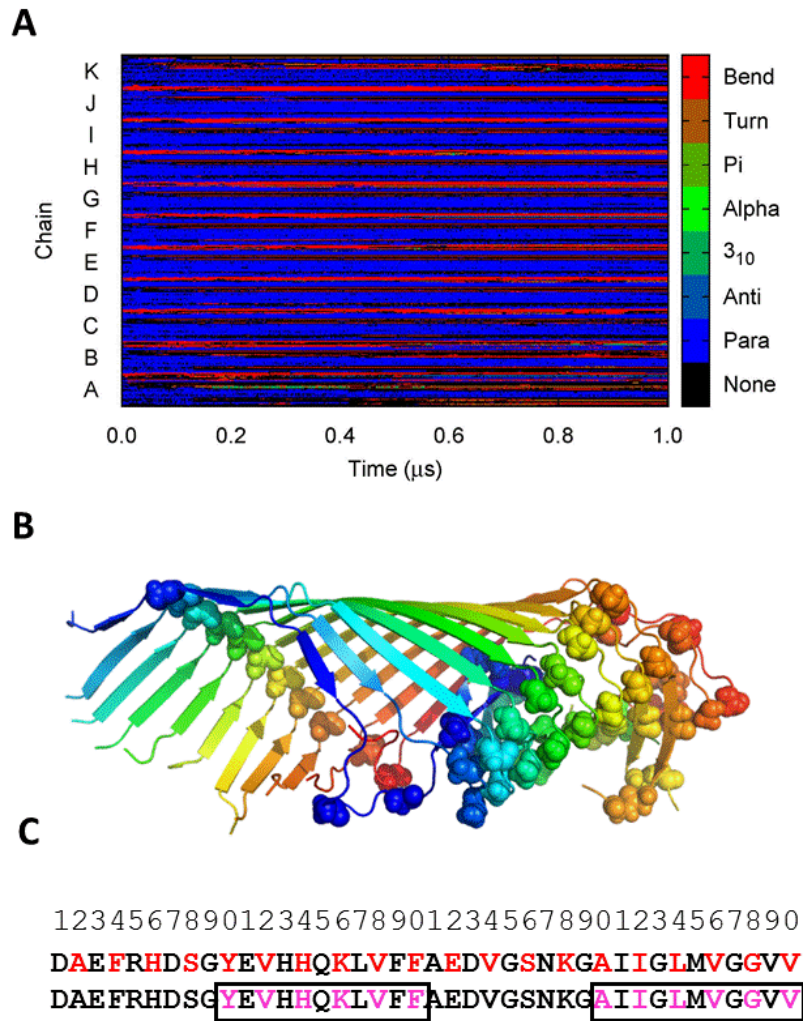is just a general indication of the phasing.

Figure 3

(A) Trajectories of C^{α} to C^{α} distances between residue 23 in chain A and residue 1 in chain J (10 strands), chain K (11 strands) or chain L (12 strands). (B) Trajectories of C^{α} to C^{α} distances between residue 40 in chain A and residue 18 in chain J, chain K or chain L.

   As mentioned in the Introduction, the experimental β-strip helix model has residues 1-18 on one side of the strip fold up to join residues 23-40 on the other side of the strip (see Figure 1). In order to monitor progress of the simulations we tracked the distance between residue 1 on one side of the strip and residue 23 on the other as well as the distance between residue 18 and residue 40. Figure 3 shows plots of these distances for all simulations. They show that in most cases these distances decrease significantly and that as confirmed by

viewing the trajectories using Pymol (www.pymol.org), folding occurs mostly within 1μs. Figure 4 (B) indicates the positions of all glycine residues. At these glycines breaks in β-sheet

15

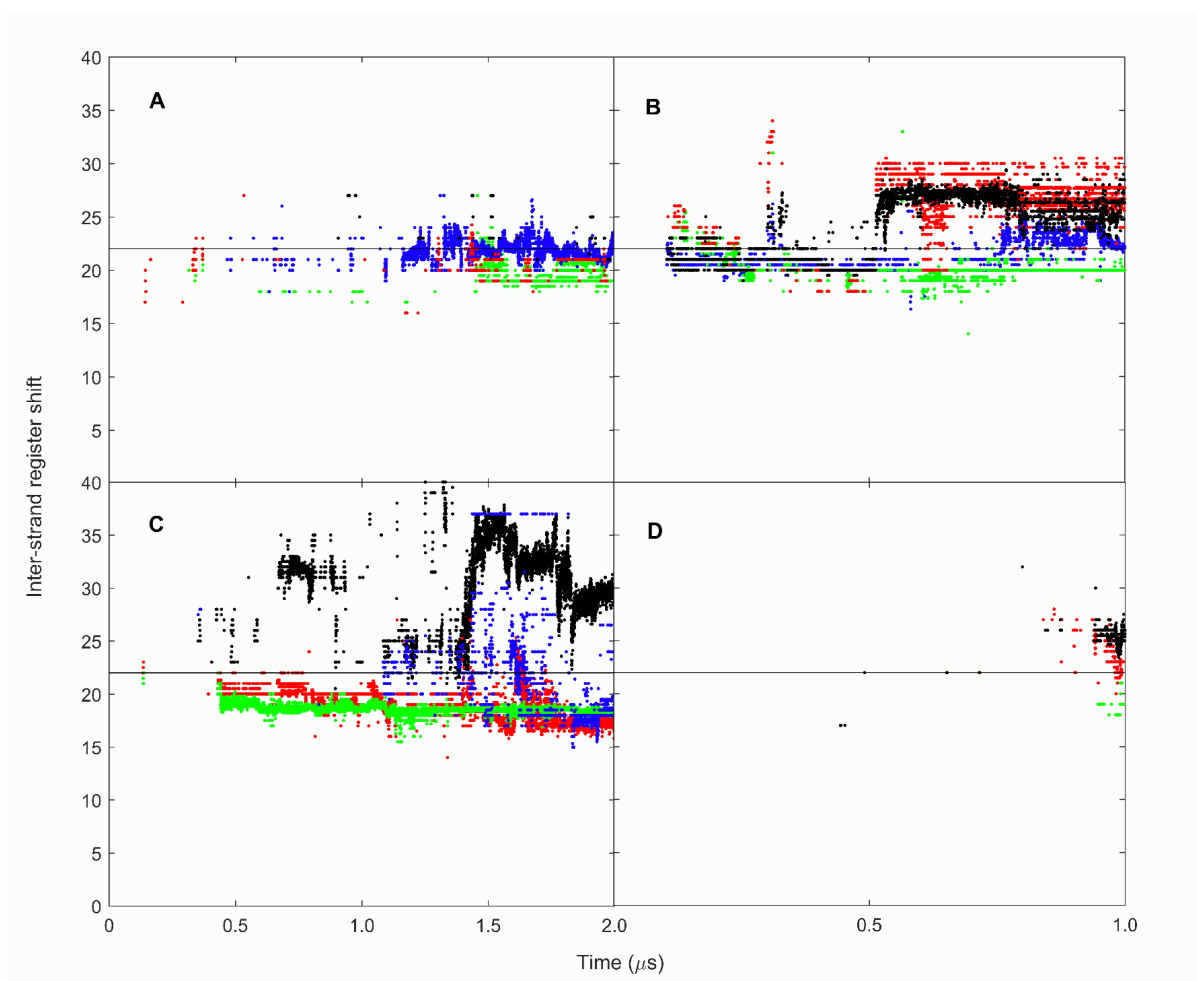hydrogen bonding and significant changes in strand direction occur, indicating that they

Figure 4

(A) Secondary structure trajectory of 11_cube_C_chg trajectory. (B) Final structure from 11_cube_C_chg trajectory showing locations of glycines in space-filling model. (C)The Aβ(40) sequence is shown indicating amino acids with side chains on the outside of the β-strip helix (red) and those on the inside (black) as determined from the simulations. The black rectangles indicate β-barrel transmembrane segments as predicted by PRED-TMBB and TMB-Pro. Magenta indicates side-chains predicted by TMB-Pro to be on the outside, i.e. on the membrane lipid side. See Discussion for further details.

Figure 5

Trajectory of inter-strand register shift between outer strands in 11-strand sheets. Black, between chain A and K, red between A and J, blue between B and K, and green between B and J. The straight horizontal line is at a register shift of 22. No points exist outside of the range shown apart from one point at an inter-strand register shift of 41 in 11_cube_C_ntl. (A) 11_cuboid_C_chg (B) 11_cube_C_chg (C) 11_cube_C_ntl (D) 11_cube_F_ntl.
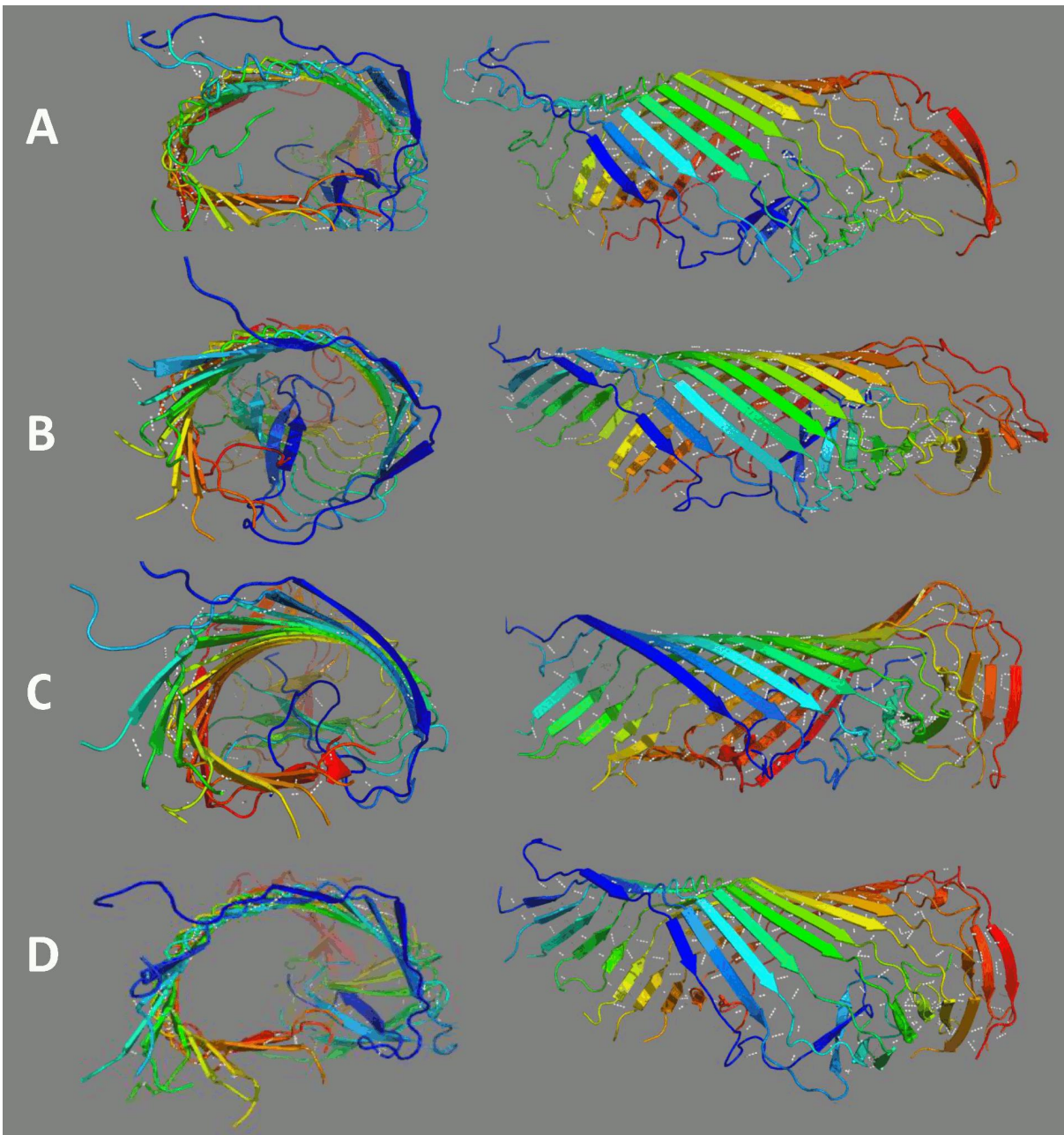
probably aid the folding process. The C-terminal end of the β-strip helix seems to fold in towards the centre of the helix as seen most clearly in Figure 6 (B) and (C). This appears to be due to there being more glycines on the C-terminal half than on the N-terminal half.

In comparison to inner strands, outer strands are more disordered and partly break away from their neighbouring strands especially at terminal regions.

Figure 5 shows trajectories of the inter-strand register shift between outer strands. It can be seen that for some simulations outer strands come into contact very early in the folding process but this is partly due to the outer strands coming away from the main strip. Overall the results show that at the end of the simulations the inter-strand register shifts are often close to, and taken together approximately centred on, the predicted register shift of 22.
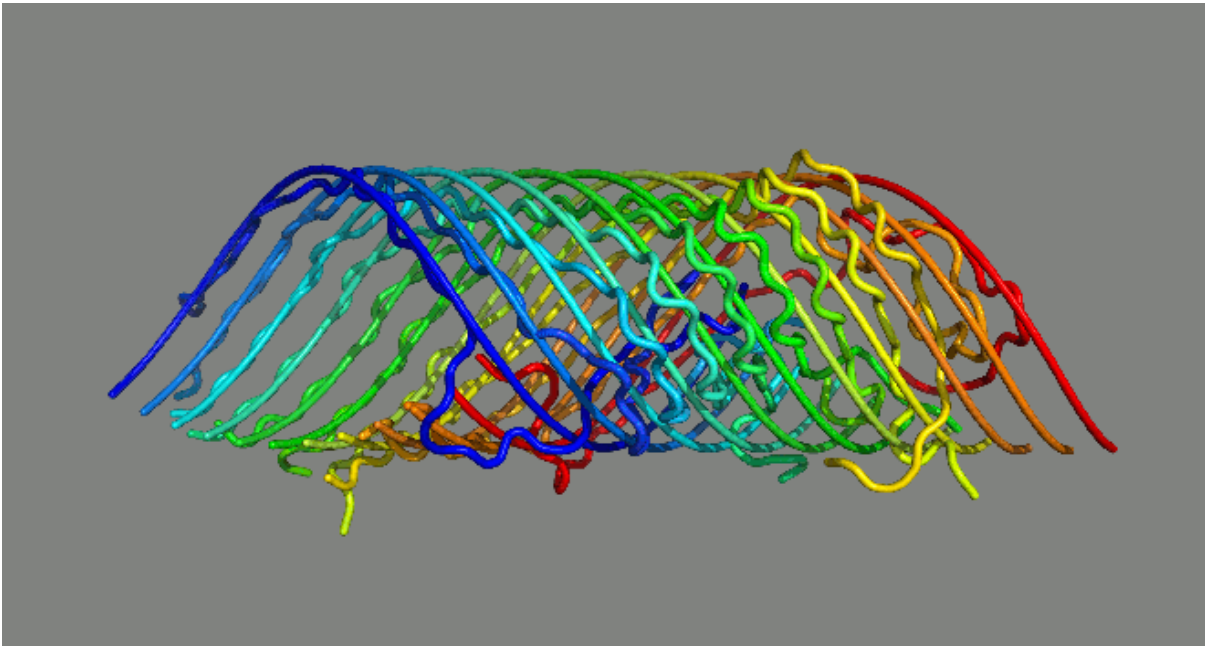
Analysis of final structures

Figure 5 shows that contacts exist between the two sides of the β-strip in the final structures. However, in an idealised β-strip helix, such as the experimental β-strip helix model, there is parallel β-sheet hydrogen bonding between the two outer strands as they join to form the β-strip helix. In none of the final structures do we find extensive hydrogen bonding between the outer strands. However, in the final structure of 11_cube_C_chg we find parallel β-sheet hydrogen bonding between Ala2 in chain B (Ala2B) and Val24K and Ser26K, which aligns Ala2B with Gly25K at a register shift of 23. In 11_cuboid_C_chg there is one hydrogen bond between Asp1B and Asp23K which is at the predicted register shift of 22. In 11_cube_C_ntl we find a single hydrogen bond between Asp8A and Val39K and in 11_cube_F_ntl there are no hydrogen bonds between the outer chains.

Figure 6

Final structures of 11-strand simulations. (A) 11_cuboid_C_chg (B) 11_cube_C_chg (C) 11_cube_C_ntl (D) 11_cube_F_ntl.

Figure 6 A-D show the final structures from all simulations with 11-strands. Although there

Figure 7

Final structure from the 11_cube_C_chg simulation and fitted β-strip helix model with $r = 15.1$ Å, $h = 65.5$ Å, $t = 22.8$ residues and $\alpha = 54.9°$. As these values are close to those of the experimental β-strip helix model ($r = 14.3$ Å, $h = 65.3$ Å, $t = 22$ residues and $\alpha = 54.0°$) it demonstrates how close the final structure is to the experimentally measured helical dimensions.

is some variation they are all similar. Their cross-sectional shapes are approximately circular but perhaps better described as elliptical with a tendency to have a "flat bottom". Table II gives the helical dimensions of the fitted β-strip models. They are remarkably close to those of the experimental β-strip helix model. In particular, for all structures, the angle α is close to the experimental value of 54.4°. Furthermore, in all simulations apart from 11_ cube_F_ntl, the width is close to experimental value which is 14-15 Å. For both 11_cube_C_chg and

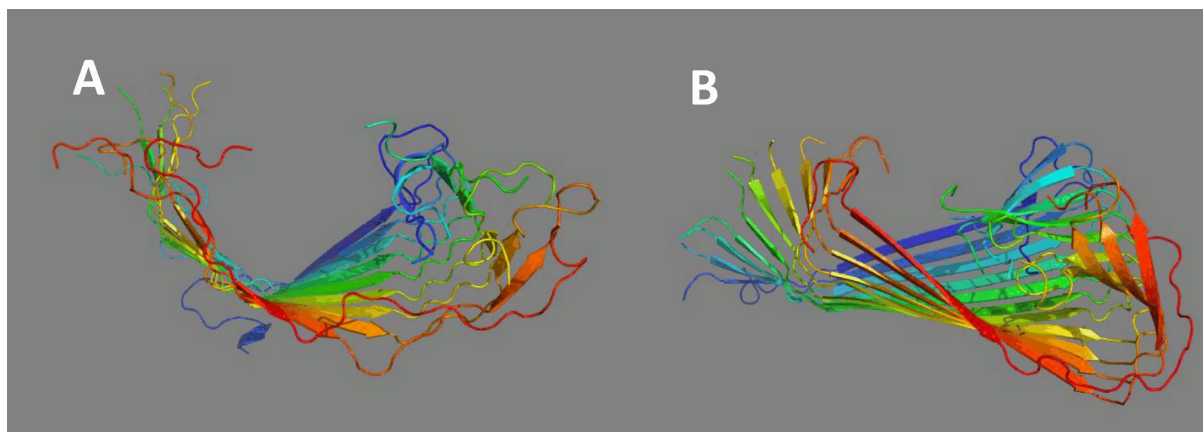11_cube_C_ntl, the height per turn, *h*, is also very close to the value for the experimental β-strip helix model.

TABLE II Helical dimensions of fitted β-strip models for final structures of 11-stranded simulations

11_exp_β-strip is the experimental β-strip helix model derived from the X-ray fibre diffraction experiments by Fraser et al. and Malinchik et al. The RMSD is between C^α atoms of the final structure and its fitted β-strip model.

Simulation name	RMSD (Å)	*r* (Å)	*h* (Å)	*α* (degrees)	*t*
11_exp_β-strip	-	14.3	65.3	54.0	22.0
11_cuboid_C_chg	8.7	16.0	76.6	52.7	21.0
11_cube_C_chg	7.7	15.1	65.5	54.9	22.8
11_cube_C_ntl	9.8	15.1	66.5	55.4	23.2
11_cube_F_ntl	8.1	17.4	83.0	52.8	21.1

Figure 7 shows the final structure of the 11_cube_C_chg simulation superposed with its fitted β-strip model. As this model is remarkably close to the experimental β-strip helix model, it effectively shows the final structure fitted with the experimental β-strip helix model. This demonstrates how close the helical dimensions of this final structure are to the experimentally measured helical dimensions. Even though our final 11-strand structure does not find support amongst the atomic resolution NMR structures, the NMR study by Ahmed et al. (Ahmed et al., 2010) on Aβ(1-42) showed that for the in-register fibril there is a close intermolecular (between different strands) interaction between Gln15 and Gly37 which corresponds to the 22 residue register shift. In the final structure of 11_cube_C_chg (the structure that most closely matches the experimental β-strip helix model) Gln15 of chain A is in contact with Gly37 of chain I (C^α- C^α distance 6.1 Å).
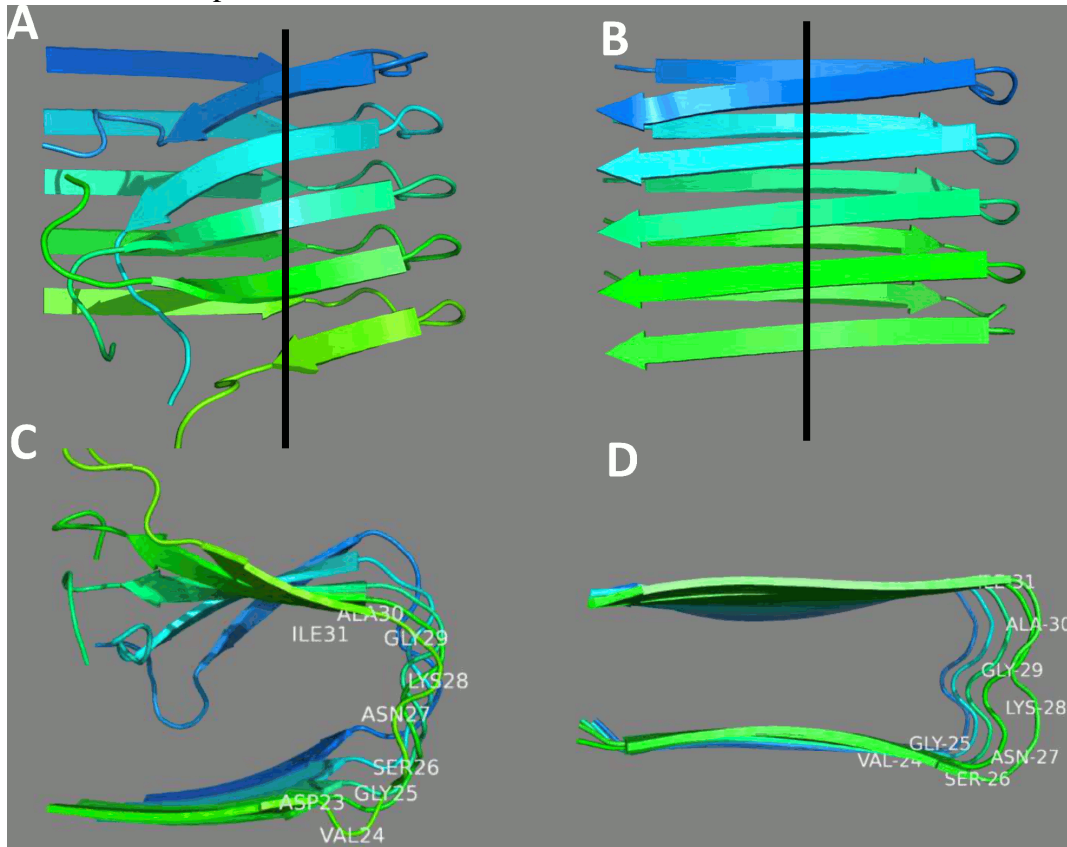
Simulations with 10- and 12-strands

Figure 8

(A) Final structure of 10_cuboid_C_chg. (B) Final structure of 12_cube_F_ntl.

10 and 12-strand sheets are not predicted to be the protofilament subunit so it would be

instructive to perform the same simulations on sheets of these sizes. For the 10-strand sheet

Figure 9

(A) Residues 17-40 chains B to F from final structure of 12_cube_F_ntl (see Figure 8 (B))

viewed perpendicular to the axis (black line) that assumes a cross-β configuration. (B) Residues

17-40 from Aβ(1-42) (PDB: 2BEG) from Lührs et al (Lührs et al., 2005) viewed perpendicular to

the axis. (C) Residues 17-40 chains B to F from final structure of 12_cube_F_ntl viewed along

axis direction. (D) Residues 17-40 from Aβ(1-42) (Lührs, et al., 2005) viewed along axis

direction.

the two sides do not come into contact, although there is contact between Lys28 on chains A and B and the C-termini of chains I and J due to the folding-in of the C-terminus end of the sheet.

For the 12-strand sheet there is little contact between the two outer strands on either side of the sheet. In fact the only contact occurs between the C-terminal of strand B and the N-terminus (His6) of strand K.

Analysis of final structures

As shown in Figure 8, it is clear from the final structures of the 10-strand and 12-strand simulations that the two outer sides do not come together. As the final structures for the 10- and 12-strand simulations are not helix-like, no fitted β-strip model was produced. The final structure of the 12-strand case is different to the 10 and 11-strand final structures. Also the individual strands are straighter. It has a flatter folded structure, reminiscent of some of the solid-state NMR structures of Aβ(1-40) or Aβ(1-42) (Lührs, et al., 2005; Petkova, Yau, & Tycko, 2006). Figure 9 shows residues 17-40, chains B to F, of the final structure of 12_cube_F_ntl in comparison with the solid-state NMR structure of Aβ(1-42) of Lührs et al. (Lührs, et al., 2005). In the NMR structure residues 1-16 are disordered but residues 17-40 are similar in structure to the corresponding region in the final structure of 12_cube_F_ntl; the loop region spans approximately the same residues, 27-30. Thus part of the 12_cube_F_ntl final structure has the characteristics of a cross-β structure. In the NMR structure there is an intra-chain salt-bridge between Asp23 and Lys28 in four out of five chains, but in the final structure only the first chain has this salt bridge. The final structure also shows a stagger, (Tycko, 2006) which forms early in the folding process and therefore seems to be related to the natural tendency for the sheet to twist.

Thus sheets of 10 and 12 strands, which are not predicted to be the protofilament subunit, do not fold to a stable helical structure.

Discussion

Assuming a β-strip helix as the protofilament building block, dimensions measured in the X-ray fibre diffraction experiments on Alzheimer Aβ(1-40) fibrils by Fraser et al. (Fraser, et al., 1992) and Malinchik et al.(Malinchik, et al., 1998) led to an experimental β-strip helix model comprising 11-strands. Our aim has been, not to simulate the folding process from an artificial structure, but rather to find support for the experimental β-strip helix model as the protofilament subunit given limited information: 11 in-register strands in a parallel β-sheet configuration. Our final structures not only resemble a β-strip helix, but they have dimensions close to those experimentally measured for the protofilament: width of ~30 Å and $\alpha \approx 54°$. Simulations on 10- and 12-strand sheets do not give rise to closed helical structures, and are not predicted for the protofilaments, which is in accord with an 11-strand model for them.

What is the significance of $t/m=2$ (or equivalently a tilt angle of 35.6°)? As shown in HMW the majority of *homomeric* β-barrels have $t/m=1$ with their strands tilted by ~55° ($\alpha=34.5°$, see Equation 1a). However, both TolC in *Ecoli* and the mycobacterial outer-membrane channel MspA also have $t/m=2$ and strands tilted by ~36° ($\alpha=54°$). In a study of non-homomeric β-barrels by Murzin et al. (Murzin, et al., 1994) where s/n (*s* being the shear number and *n* the number of strands forming the barrel) is the equivalent of t/m, the significance of $s/n=1$ and $s/n=2$ was attributed to residues in the interior of the barrel forming "*symmetrical layers in planes perpendicular to its axis*" whereas for barrels where $1<s/n<2$ "*packing is more complicated*". They also argued that barrels with $s/n<1$ and $s/n>2$ would only be stable for "*very special combinations of side-chains and therefore expected to be rare*
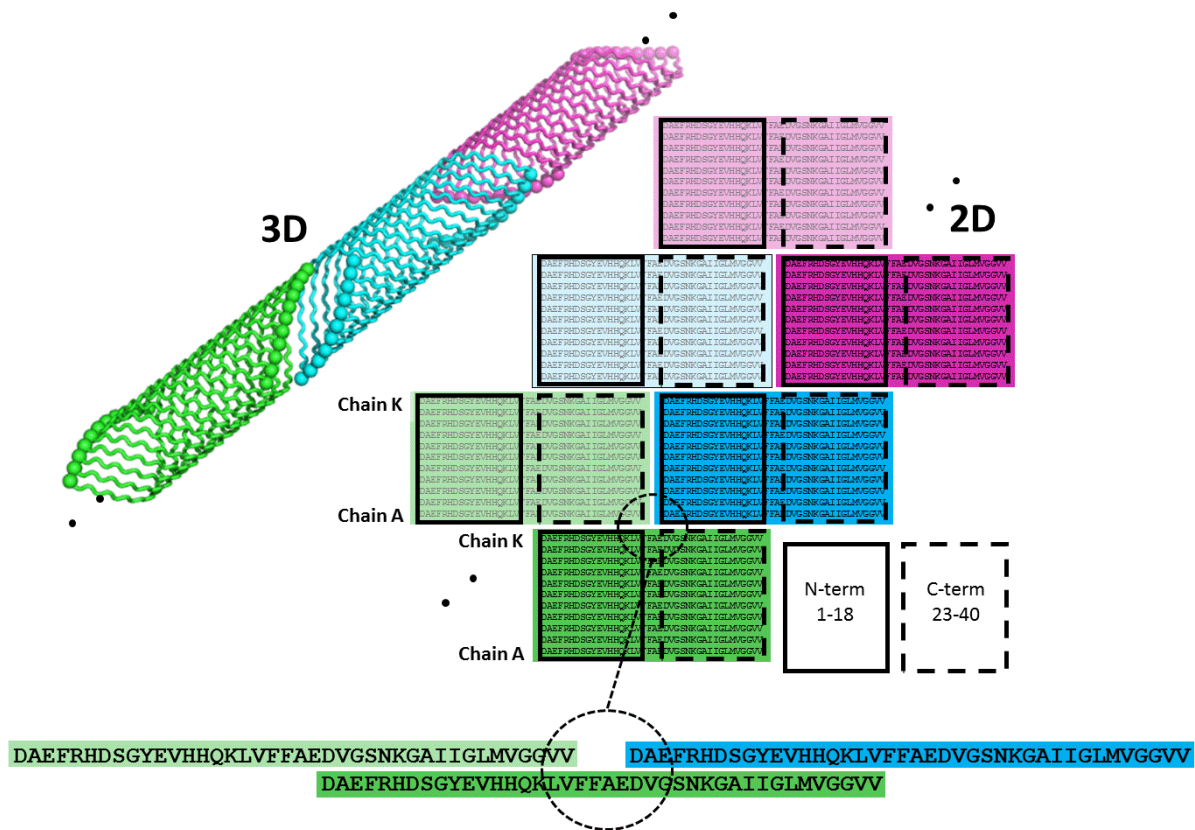
or not to occur". Thus *t/m*=2 is significant as it corresponds to a tilt angle that produces favourable side-chain packing.

The ability of small oligomers of Aβ(1-40) to form ion-channels within membranes (Arispe, Pollard, & Rojas, 1993) and their consequential toxicity motivated Jang et al. (Jang, et al., 2010) to use solid-state NMR structures (Lührs, et al., 2005; Petkova, et al., 2006) to build β-barrel-like structures with a tilt of 37° that resemble atomic force microscopy images of Aβ oligomers in membranes. The significance of our result is that our 11-strand β-strip helix is a β-barrel-like structure with a tilt of 35° that is close in structure to the 12-strand membrane-embedded β-barrel from TolC in *Ecoli* (width 31 Å, $\alpha = 54°$; see Figure 2 in HMW). The transmembrane β-barrel prediction programs TMBpro (Randall, Cheng, Sweredoski, & Baldi, 2008) and PRED-TMBB (Bagos, Liakopoulos, Spyropoulos, & Hamodrakas, 2004) were used to analyse the Aβ(1-40) sequence to see if it had the expected properties of known β-barrels. As solved transmembrane β-barrels are antiparallel and these programs are designed for a single monomers, they are not ideally suited for this case. However, they can help predict the regions in the Aβ(1-40) sequence that have a propensity to form a transmembrane β-strands. Figure 4(C) shows two regions of 10 residues each, which are predicted by both programs to be transmembrane β-strands. These regions have a 9-residue overlap in the β-strip helix forming a large continuous portion of the whole β-strip helix. Within these segments the side-chains predicted by TMB-pro to be on the membrane side correspond to those on the outside of the β-strip helices from the simulations.

The cross-β structure has become the established configuration for the amyloid fibril so it is important to be able to reconcile the proposed β-strip helix structure with the cross-β structure. The final structure of the 12-strand simulation might provide a clue. The conformation of β-strand-loop-β-strand found in the 12-strand structure has a stagger similar to that seen in some atomic resolution NMR structures. The stagger here seems to arise from

the natural tendency for a β-sheet to twist but this stagger is much larger in the 11-strand case allowing the opposite sides of the sheet to come into contact at a register shift of 22 to form a closed structure. In the 12-strand case the two sides of the sheet are not able to come into contact and the final structure may then form protofilaments that are closer to the cross-β configuration. Therefore, a variety of protofilament strains could arise from a heterogeneous "soup" of partially folded β-sheets each comprising differing numbers of strands. The strain of protofilament that arises would depend on environmental conditions.

Figure 10 shows β-strip helices - each an experimental β-strip helix model - as

protofilament subunits joining end-to-end. An attractive feature of the β-strip helix as a

Figure 10

2D and 3D depiction of β-strip helix (each acting as a protofilament subunit) stabilisation and association. The 2D depiction shows the register shift as an association of the N-terminal sequence segment (1-18) and the C-terminal sequence segment (23-40) from opposite sides of the same β-strip helix (each *single* strip is depicted twice in the same colour, once in bold and once in faint) and between adjacent β-strip helices (neighbouring strips of different colour). The 3D depiction shows experimental β-strip helix models joining end-to-end, the modelling of which is described in Supplementary Material. The N- and C-terminal ends are depicted as spheres to help show the slot between neighbouring subunits. The Aβ(40) sequence is shown illustrating the register shift.

protofilament subunit, is it shows how protofilament subunits join together end-to-end via the

association of the same sequence segments as those that come together to stabilise an

individual β-strip helix. In the 2D representation of Figure 10 one can see that the association

of the N-terminal segment of chain K and the C-terminal segment of chain A stabilises the

individual β-strip helices, each a protofilament subunit. This leaves the C-terminal segment

of chain K to associate with the N-terminal segment of chain A of the next protofilament subunit, and the N-terminal segment of chain A to associate with the C-terminal segment of chain K of the previous protofilament subunit. In all these associations 18-residue sequence segments at a register shift of 22 come together. This model suggests a seeding effect and that protofilaments grow in both directions. The same principle appears to apply in the HETs(218–289) infectious form of the prion protein, (Wasmer, et al., 2008) which is formed from single-strand β-helices joining end-to-end. HET-s(218–289) has 21-residue tandem pseudo repeat sequences spaced by 15 residues brought into alignment by a register shift of 36 stabilising individual β-helix subunits and the join between subunits (see Figure 7(A) in HMW for 2D and 3D depictions of this for HET-s(218–289)).

With $L = 40$ and $t = 22$ the condition $L \leq 2t \leq 2(L\text{-}1)$ is satisfied and with $g = 5$ the resulting gap is long enough to provide the necessary space for the N- and C-terminal groups. Figure 10 depicts the protofilament as an association of β-strip helices joining end-to-end as protofilament subunits.

In the models suggested by Malinchik et al. on the basis of X-ray fibre diffraction and electron microscopy experiments, a fibril comprises 3-5 protofilaments. Protofilaments are likely to be intertwining due a natural propensity for β-helices to twist, as seen for example in the T4 phage spike. Thus in this model a fibril is likely to have a number of structural features combining those of individual protofilaments with those arising from protofilament intertwining.

The proposed β-strip helix is a structure that combines qualities of both β-helices and β-barrels. Its resemblance to transmembrane β-barrels such as that found in TolC might explain why small oligomers of Alzheimer Aβ(1-40) are able to form toxic ion channels. Its

β-helix-like quality could explain how, like the β-helix in the HET-s(218–289) prion protein, these small oligomers join together to form protofilaments.

Acknowledgements

References

Ahmed, M., Davis, J., Aucoin, D., Sato, T., Ahuja, S., Aimoto, S., . . . Smith, S. O. (2010). Structural conversion of neurotoxic amyloid-beta(1-42) oligomers to fibrils. *Nature Structural & Molecular Biology, 17*(5), pp. 561-U556. doi:10.1038/nsmb.1799 Retrieved from <Go to ISI>://WOS:000277330700008

Arispe, N., Pollard, H. B., & Rojas, E. (1993). Giant multilevel cation channels formed by alzheimer-disease amyloid beta-protein Abeta-p-(1-40) in bilayer-membranes. *Proceedings of the National Academy of Sciences of the United States of America, 90*(22), pp. 10573-10577. doi:10.1073/pnas.90.22.10573 Retrieved from <Go to ISI>://WOS:A1993MH32200034

Bagos, P. G., Liakopoulos, T. D., Spyropoulos, I. C., & Hamodrakas, S. J. (2004). PRED-TMBB: a web server for predicting the topology of beta-barrel outer membrane proteins. Nucleic Acids Research, 32, W400-W404. doi: 10.1093/nar/gkh417

Barz, B., Olubiyi, O. O., & Strodel, B. (2014). Early amyloid beta-protein aggregation precedes conformational change. *Chemical Communications, 50*(40), pp. 5373-5375. doi:10.1039/c3cc48704k Retrieved from <Go to ISI>://WOS:000335011200066

Berendsen, H. J. C., Postma, J. P. M., van Gunsteren, W. F., Di Nola, A., & Haak, J. R. (1984). Molecular-Dynamics with Coupling to an External Bath. *Journal of Chemical Physics, 81*(8), pp. 3684-3690. Retrieved from <Go to ISI>://WOS:A1984TQ73500045

Buxbaum, J. N., & Linke, R. P. (2012). A Molecular History of the Amyloidoses. *Journal of Molecular Biology, 421*(2-3), pp. 142-159. doi:10.1016/j.jmb.2012.01.024 Retrieved from <Go to ISI>://WOS:000306885200002

Coles, M., Bicknell, W., Watson, A. A., Fairlie, D. P., & Craik, D. J. (1998). Solution structure of amyloid beta-peptide(1-40) in a water-micelle environment. Is the membrane-spanning domain where we think it is? Biochemistry, 37(31), pp. 11064-11077. doi:10.1021/bi972979f Retrieved from <Go to ISI>://WOS:000075397000025

D.A. Case, R. M. B., D.S. Cerutti, T.E. Cheatham, III, T.A. Darden, R.E. Duke, T.J. Giese, H. Gohlke,, A.W. Goetz, N. H., S. Izadi, P. Janowski, J. Kaus, A. Kovalenko, T.S. Lee, S. LeGrand, P. Li, C., Lin, T. L., R. Luo, B. Madej, D. Mermelstein, K.M. Merz, G. Monard, H. Nguyen, H.T. Nguyen, I., Omelyan, A. O., D.R. Roe, A. Roitberg, C. Sagui, C.L. Simmerling, W.M. Botello-Smith, J. Swails,, & R.C. Walker, J. W., R.M. Wolf, X. Wu, L. Xiao and P.A. Kollman. (2016). AMBER 2016: University of California, San Francisco.

Eisenberg, D., & Jucker, M. (2012). The amyloid state of proteins in human diseases. *Cell, 148*(6), pp. 1188-1203. doi:10.1016/j.cell.2012.02.022 Retrieved from <Go to ISI>://WOS:000301889500016

Essmann, U., Perera, L., Berkowitz, M. L., Darden, T., Lee, H., & Pedersen, L. G. (1995). A smooth particle mesh Ewald method. *Journal of Chemical Physics, 103*(19), pp. 8577-8593. Retrieved from <Go to ISI>://WOS:A1995TE36400026

Fraser, P. E., Nguyen, J. T., Inouye, H., Surewicz, W. K., Selkoe, D. J., Podlisny, M. B., & Kirschner, D. A. (1992). Fibril formation by primate, rodent, and Dutch-hemorrhagic analogs of Alzheimer amyloid beta-protein. *Biochemistry, 31*(44), pp. 10716-10723. doi:10.1021/bi00159a011 Retrieved from <Go to ISI>://WOS:A1992JX83700011

Gotz, A. W., Williamson, M. J., Xu, D., Poole, D., Le Grand, S., & Walker, R. C. (2012). Routine microsecond molecular dynamics simulations with AMBER on GPUs. 1. Generalized Born. *Journal of Chemical Theory and Computation, 8*(5), pp. 1542-1555. Retrieved from <Go to ISI>://WOS:000303628400004

Hayward, S., & Milner-White, E. J. (2011). Simulation of the beta- to alpha-sheet transition results in a twisted sheet for antiparallel and an alpha-nanotube for parallel strands: Implications for amyloid formation. *Proteins, 79*(11), pp. 3193-3207. doi:10.1002/prot.23154 Retrieved from <Go to ISI>://WOS:000296705200015

Hayward, S., & Milner-White, E. J. (2017). Cover Image, Volume 85, Issue 10. *Proteins, 85*(10), pp. C1-C1. doi:10.1002/prot.25141 Retrieved from

Hayward, S., & Milner-White, E. J. (2017). Geometrical principles of homomeric β-barrels and β-helices: Application to modeling amyloid protofilaments. *Proteins, 85*(10), pp. 1866-1881. doi:10.1002/prot.25341

Jang, H., Arce, F. T., Ramachandran, S., Capone, R., Lal, R., & Nussinov, R. (2010). Beta-barrel topology of Alzheimer's beta-amyloid ion channels. *Journal of Molecular*

Biology, 404(5), pp. 917-934. doi:10.1016/j.jmb.2010.10.025 Retrieved from <Go to ISI>://WOS:000285657800014

Joung, I. S., & Cheatham, T. E. (2008). Determination of alkali and halide monovalent ion parameters for use in explicitly solvated biomolecular simulations. *Journal of Physical Chemistry B, 112*(30), pp. 9020-9041. Retrieved from <Go to ISI>://WOS:000257926800026

Krivov, G. G., Shapovalov, M. V., & Dunbrack, R. L. (2009). Improved prediction of protein side-chain conformations with SCWRL4. *Proteins, 77*(4), pp. 778-795. doi:10.1002/prot.22488 Retrieved from <Go to ISI>://WOS:000271602000003

Le Grand, S., Gotz, A. W., & Walker, R. C. (2013). SPFP: Speed without compromise-A mixed precision model for GPU accelerated molecular dynamics simulations. *Computer Physics Communications, 184*(2), pp. 374-380. Retrieved from <Go to ISI>://WOS:000311661100012

Lendel, C., Bjerring, M., Dubnovitsky, A., Kelly, R. T., Filippov, A., Antzutkin, O. N., . . . Hard, T. (2014). A hexameric peptide barrel as building block of amyloid-beta protofibrils. *Angewandte Chemie-International Edition, 53*(47), pp. 12756-12760. doi:10.1002/anie.201406357 Retrieved from <Go to ISI>://WOS:000344793400011

Lu, J. X., Qiang, W., Yau, W. M., Schwieters, C. D., Meredith, S. C., & Tycko, R. (2013). Molecular structure of beta-amyloid fibrils in Alzheimer's disease brain tissue. *Cell, 154*(6), pp. 1257-1268. doi:10.1016/j.cell.2013.08.035 Retrieved from <Go to ISI>://WOS:000324239300015

Lührs, T., Ritter, C., Adrian, M., Riek-Loher, D., Bohrmann, B., Döbeli, H., . . . Riek, R. (2005). 3D structure of Alzheimer's amyloid-beta(1-42) fibrils. *Proceedings of the National Academy of Sciences of the United States of America, 102*(48), pp. 17342-

17347. doi:10.1073/pnas.0506723102 Retrieved from <Go to ISI>://WOS:000233762000016

Maier, J. A., Martinez, C., Kasavajhala, K., Wickstrom, L., Hauser, K. E., & Simmerling, C. (2015). ff14SB: Improving the accuracy of protein side chain and backbone parameters from ff99SB. *J Chem Theory Comput, 11*(8), pp. 3696-3713. doi:10.1021/acs.jctc.5b00255 Retrieved from https://www.ncbi.nlm.nih.gov/pubmed/26574453

Makin, O. S., & Serpell, L. C. (2005). Structures for amyloid fibrils. [Review]. *Febs Journal, 272*(23), pp. 5950-5961. doi:10.1111/j.1742-4658.2005.05025.x Retrieved from <Go to ISI>://WOS:000233314300003

Malinchik, S. B., Inouye, H., Szumowski, K. E., & Kirschner, D. A. (1998). Structural analysis of Alzheimer's beta(1-40) amyloid: Protofilament assembly of tubular fibrils. *Biophysical Journal, 74*(1), pp. 537-545. Retrieved from <Go to ISI>://WOS:000073393400053

McLachlan, A. D. (1979). Gene duplications in the structural evolution of chymotrypsin. *Journal of Molecular Biology, 128*(1), pp. 49-&. doi:10.1016/0022-2836(79)90308-5 Retrieved from <Go to ISI>://WOS:A1979GK47000003

Murzin, A. G., Lesk, A. M., & Chothia, C. (1994). Principles determining the structure of beta-sheet barrels in proteins .1. A theoretical-analysis. *Journal of Molecular Biology, 236*(5), pp. 1369-1381. doi:10.1016/0022-2836(94)90064-7 Retrieved from <Go to ISI>://WOS:A1994NA30200010

Nasica-Labouze, J., Nguyen, P. H., Sterpone, F., Berthoumieu, O., Buchete, N. V., Cote, S., . . . Derreumaux, P. (2015). Amyloid beta protein and Alzheimer's disease: When computer simulations complement experimental studies. *Chemical Reviews, 115*(9),

pp. 3518-3563. doi:10.1021/cr500638n Retrieved from <Go to ISI>://WOS:000354906800009

Paravastu, A. K., Leapman, R. D., Yau, W. M., & Tycko, R. (2008). Molecular structural basis for polymorphism in Alzheimer's beta-amyloid fibrils. *Proceedings of the National Academy of Sciences of the United States of America, 105*(47), pp. 18349-18354. doi:10.1073/pnas.0806270105 Retrieved from <Go to ISI>://WOS:000261489300057

Petkova, A. T., Ishii, Y., Balbach, J. J., Antzutkin, O. N., Leapman, R. D., Delaglio, F., & Tycko, R. (2002). A structural model for Alzheimer's beta-amyloid fibrils based on experimental constraints from solid state NMR. *Proceedings of the National Academy of Sciences of the United States of America, 99*(26), pp. 16742-16747. doi:10.1073/pnas.262663499 Retrieved from <Go to ISI>://WOS:000180101600044

Petkova, A. T., Yau, W. M., & Tycko, R. (2006). Experimental constraints on quaternary structure in Alzheimer's beta-amyloid fibrils. *Biochemistry, 45*(2), pp. 498-512. Retrieved from <Go to ISI>://000234656700016

Randall, A., Cheng, J. L., Sweredoski, M., & Baldi, P. (2008). TMBpro: secondary structure, beta-contact and tertiary structure prediction of transmembrane beta-barrel proteins. Bioinformatics, 24(4), 513-520. doi: 10.1093/bioinformatics/btm548

Ritter, C., Maddelein, M. L., Siemer, A. B., Lührs, T., Ernst, M., Meier, B. H., . . . Riek, R. (2005). Correlation of structural elements and infectivity of the HET-s prion. *Nature, 435*(7043), pp. 844-848. doi:10.1038/nature03793 Retrieved from <Go to ISI>://WOS:000229638700056

Rodriguez, J. A., Ivanova, M. I., Sawaya, M. R., Cascio, D., Reyes, F. E., Shi, D., . . . Eisenberg, D. S. (2015). Structure of the toxic core of alpha-synuclein from invisible

crystals. *Nature, 525*(7570), pp. 486-490. doi:10.1038/nature15368 Retrieved from

<Go to ISI>://WOS:000361599900043

Sawaya, M. R., Sambashivan, S., Nelson, R., Ivanova, M. I., Sievers, S. A., Apostol, M. I., . .

. Eisenberg, D. (2007). Atomic structures of amyloid cross-beta spines reveal varied

steric zippers. *Nature, 447*(7143), pp. 453-457. doi:10.1038/nature05695 Retrieved

from <Go to ISI>://WOS:000246693100042

Serra-Batiste, M., Ninot-Pedrosa, M., Bayoumi, M., Gairi, M., Maglia, G., & Carulla, N.

(2016). A beta 42 assembles into specific beta-barrel pore-forming oligomers in

membrane-mimicking environments. *Proceedings of the National Academy of

Sciences of the United States of America, 113*(39), pp. 10866-10871.

doi:10.1073/pnas.1605104113 Retrieved from <Go to ISI>://WOS:000383954700039

Shewmaker, F., McGlinchey, R. P., & Wickner, R. B. (2011). Structural insights into

functional and pathological amyloid. *Journal of Biological Chemistry, 286*(19), pp.

16533-16540. doi:10.1074/jbc.R111.227108 Retrieved from <Go to

ISI>://WOS:000290301900001

Shinchuk, L. M., Sharma, D., Blondelle, S. E., Reixach, N., Inouye, H., & Kirschner, D. A.

(2005). Poly-(L-alanine) expansions form core beta-sheets that nucleate amyloid

assembly. *Proteins, 61*(3), pp. 579-589. doi:10.1002/prot.20536 Retrieved from <Go

to ISI>://WOS:000233029800014

Sindhikara, D. J., Kim, S., Voter, A. F., & Roitberg, A. E. (2009). Bad seeds sprout perilous

dynamics: Stochastic thermostat induced trajectory synchronization in biomolecules.

Journal of Chemical Theory and Computation, 5(6), pp. 1624-1631. Retrieved from

<Go to ISI>://WOS:000266865000017

Sipe, J. D., & Cohen, A. S. (2000). Review: History of the amyloid fibril. *Journal of Structural Biology, 130*(2-3), pp. 88-98. doi:10.1006/jsbi.2000.4221 Retrieved from <Go to ISI>://WOS:000089022900002

Takemura, K., & Kitao, A. (2012). Water model tuning for improved reproduction of rotational diffusion and NMR spectral density. *Journal of Physical Chemistry B, 116*(22), pp. 6279-6287. Retrieved from <Go to ISI>://WOS:000304888600005

http://pubs.acs.org/doi/pdfplus/10.1021/jp301100g

Tofoleanu, F., Brooks, B. R., & Buchete, N. V. (2015). Modulation of Alzheimer's A beta Protofilament-Membrane Interactions by Lipid Headgroups. *ACS Chemical Neuroscience, 6*(3), pp. 446-455. doi:10.1021/cn500277f Retrieved from <Go to ISI>://WOS:000351419900013

Torok, M., Milton, S., Kayed, R., Wu, P., McIntire, T., Glabe, C. G., & Langen, R. (2002). Structural and dynamic features of Alzheimer's Abeta peptide in amyloid fibrils studied by site-directed spin labeling. *Journal of Biological Chemistry, 277*(43), pp. 40810-40815. doi:10.1074/jbc.M205659200 Retrieved from <Go to ISI>://WOS:000178791400084

Toyama, B. H., & Weissman, J. S. (2011). Amyloid structure: Conformational diversity and consequences. In R. D. Kornberg, C. R. H. Raetz, J. E. Rothman & J. W. Thorner (Eds.), *Annual Review of Biochemistry, Vol 80* (Vol. 80, pp. 557-585).

Tycko, R. (2006). Molecular structure of amyloid fibrils: insights from solid-state NMR. *Quarterly Reviews of Biophysics, 39*(1), pp. 1-55. doi:10.1017/s0033583506004173 Retrieved from <Go to ISI>://WOS:000241450300001

Wasmer, C., Lange, A., van Melckebeke, H., Siemer, A. B., Riek, R., & Meier, B. H. (2008). Amyloid fibrils of the HET-s(218-289) prion form a beta solenoid with a triangular

hydrophobic core. *Science, 319*(5869), pp. 1523-1526. doi:10.1126/science.1151839

Retrieved from <Go to ISI>://WOS:000253943800038

Wickner, R. B., Shewmaker, F., Kryndushkin, D., & Edskes, H. K. (2008). Protein

inheritance (prions) based on parallel in-register beta-sheet amyloid structures.

Bioessays, 30(10), pp. 955-964. doi:10.1002/bies.20821 Retrieved from <Go to

ISI>://WOS:000259959700007